EEET ECOLOGICAL ENGINEERING & ENVIRONMENTAL TECHNOLOGY

Ecological Engineering & Environmental Technology, 2026, 27(7), 216–234
https://doi.org/10.12912/27197050/223923
ISSN 2719–7050, License CC-BY 4.0

Received: 2026.05.24
Accepted: 2026.06.15
Published: 2026.07.01

Zinc sulfate-induced oxidative stress and exploratory CMIP6-linked vulnerability assessment in durum wheat (*Triticum durum* Desf.) varieties from northern Algeria

Zahia Guediri[1*], Nadia Nawel Azizi[2], Ibtissem Samai[3], Nesrine Hacini[2], Amir Brinis[1], Mohamed Nejib El Melki[4]

[1] Plant Breeding Laboratory, Faculty of Sciences, Badji Mokhtar University, Annaba, Algeria
[2] Laboratory of Functional and Evolutionary Ecology Research, Faculty of Nature and Life Sciences, Chadli Bendjedid University of El Tarf, El-Tarf 36000, Algeria
[3] Laboratory Research of Soil and Sustainable Development, Department of Biology, Faculty of Sciences, Badji Mokhtar University, Annaba, Algeria
[4] Higher School of Engineers of Medjez El Bab, Department of Mechanical and Agro-Industrial Engineering, University of Jendouba, Jendouba 8189, Tunisia, Algeria
* Corresponding author's e-mail: zahia.guediri@univ-annaba.dz

ABSTRACT

Zinc contamination, combined with accelerating climate change, represents a major constraint to durum wheat cultivation in Algeria. Two contrasting *Triticum durum* varieties, Simeto and Ammar 6, were evaluated under four $ZnSO_4$ concentrations using the raw replicate-level dataset provided for this revision (2 varieties × 4 doses × 3 biological replicates). The revised analysis integrates ANOVA, multivariate statistics, dose-response modelling and an exploratory CMIP6-linked vulnerability framework. The recalculated results confirm clear variety × treatment interactions for several traits. Ammar 6 maintained higher germination under zinc exposure and showed strong biomass accumulation, especially for aerial dry mass at D200, whereas Simeto showed a more complex trait-dependent response at D150 rather than a perfect D100–D150 plateau. Catalase activity was treated as a LOD/LOQ-censored low-level response: Ammar 6 at D0 and D100 was reported as <LOD, and values between LOD and LOQ were considered detected but below quantification and interpreted only qualitatively. The CMIP6/Bayesian component is presented as exploratory uncertainty propagation using equal central CSI weights ($\alpha = 0.5$, $\gamma = 0.5$), not as a field-validated prediction. These findings support the use of raw-data-based varietal screening while emphasizing the need for larger replicate numbers and field validation under natural zinc gradients. The greenhouse experiment used three true biological replicates per variety x dose combination; the very small within-cell standard deviations are reported transparently and are not used to overstate certainty. The CMIP6/Bayesian component is therefore framed strictly as a hypothesis-generating vulnerability extrapolation, because zinc dose-response functions were not validated experimentally under temperature or precipitation stress.

Keywords: *Triticum durum*; zinc toxicity; oxidative stress; abiotic stress tolerance; CMIP6.

INTRODUCTION

Durum wheat (*Triticum durum* Desf.) is a strategic crop in Algeria. It occupies more than 1.5 million hectares in the Algerian Tell and provides the main raw material for semolina, pasta, and couscous consumed by a population of approximately 45 million. Grain and semolina quality, particularly protein content, gluten strength, and yellow pigment concentration, determine suitability for pasta and couscous processing. Despite varietal improvement efforts by the Technical Institute for Field Crops since the 1990s (Kellou et al., 2023; Trifa et al., 2024), Algeria still imports nearly half of its durum wheat requirements because of persistent structural yield gaps, making

the improvement of local productivity a national priority (FAO, 2023; ONS, 2023).

Durum wheat production is increasingly threatened by soil zinc contamination and climate change. Zinc contamination originates mainly from irrigation with industrial waste+water, phosphate fertilizer inputs, and atmospheric deposition near mining and industrial areas. At excessive concentrations, zinc induces oxidative stress through the overproduction of reactive oxygen species, disrupting nutrient uptake, inhibiting germination-related enzymes, destabilising membranes, and damaging proteins, lipids, and DNA (Hasanuzzaman et al., 2020; Zang et al., 2021). In Algerian peri-industrial zones, zinc concentrations in soil solution can reach 150–400 μmol L^{-1}, supporting the experimental $ZnSO_4$ range used in this study.

Climate projections indicate that the Mediterranean region is warming faster than the global average, with North Africa expected to experience higher temperatures and reduced rainfall (Chetioui and Bouregaa, 2024; O'Neill et al., 2016). These trends may intensify water deficit, increase metal accumulation in soils, and further reduce cereal productivity. For example, irrigation water demand is projected to rise by 7.7–17.2%, while rainfed durum wheat yield losses of 8–32% are expected under future climate scenarios (Benmahammed et al., 2022; Faye et al., 2025).

Plants respond to zinc-induced abiotic stress through a coordinated antioxidant defense system. Enzymatic defenses, including catalase, peroxidase, superoxide dismutase, and ascorbate peroxidase, detoxify reactive oxygen species, whereas non-enzymatic defenses rely on osmoprotectants such as free proline and soluble sugars (Gill and Tuteja, 2010; Hasanuzzaman et al., 2020). Induced tolerance is activated after stress exposure, whereas constitutive tolerance involves continuous osmoprotectant production. Under severe heavy metal stress, antioxidant enzymes can become inactivated, a process commonly referred to as antioxidant enzyme collapse (Rizwan et al., 2019; Zang et al., 2021). Roots act as the primary detoxification barrier, which justifies the use of root and shoot dry mass slopes as variety-specific sensitivity parameters (Leksir and Chenchouni, 2023; Li et al., 2013).

Most studies on climate impacts in Algeria have focused on general yield trends without distinguishing varietal responses or considering combined stress conditions (Alsafadi et al., 2023; Benmahammed et al., 2022). Therefore, there is a need to integrate variety-specific physiological responses to zinc stress with probabilistic climate projections to better guide adaptation strategies for Algerian cereal production. This study combines controlled $ZnSO_4$ stress trials with climate projections under SSP2-4.5 and SSP3-7.0 scenarios (Chetioui and Bouregaa, 2024; O'Neill et al., 2016). Building on climate suitability approaches such as the AHP-weighted climatic suitability index (Alsafadi et al., 2023), we develop a coupled vulnerability index (CVI) that incorporates variety-specific dose-response slopes and Bayesian posterior probabilities. We hypothesise that Ammar 6 is less sensitive than Simeto to zinc-induced heavy metal stress, that the two varieties use distinct antioxidant defense strategies, and that the adaptive advantage of Ammar 6 increases under more severe climate scenarios. Because the climate component was not tested as a factorial temperature x zinc experiment, the study tests a controlled ZnSO4 tolerance hypothesis and explores how this varietal ranking might propagate under standardized CMIP6 climate anomalies; it does not claim direct prediction of future field yield.

MATERIALS AND METHODS

Methodological approach

This study was based on an integrated and hierarchical framework designed to assess the sensitivity of two durum wheat varieties (*Simeto* and *Ammar 6*) to zinc-induced metal stress, and to project their behaviour under future climatic conditions. The methodology combines three complementary levels: a controlled greenhouse experiment, statistical modelling of biological responses, and coupling with climate projections within a coherent framework linking plant responses to anticipated environmental constraints.

The first step consisted of a greenhouse experiment designed to characterise the physiological, biochemical, and agronomic responses of the two varieties exposed to an increasing zinc-stress gradient. This controlled design made it possible to isolate genotype-specific tolerance mechanisms and to quantify the magnitude of inter-varietal variation.

The experimental data were then analysed using multivariate statistical methods in order to identify synthetic indicators of varietal

sensitivity. Dose response models were fitted for each measured trait, producing coefficients that quantitatively describe the responsiveness of biological traits to stress intensity. These coefficients were interpreted as intrinsic descriptors of varietal physiological functioning, analogous to genotypic parameters used in crop models (Tardieu, 2013).

These coefficients were subsequently used to construct biological response functions describing the dynamic behaviour of the varieties under abiotic constraints. This formalisation goes beyond a purely descriptive interpretation and enables transposition to varied environmental conditions, including future ones.

In this perspective, the response functions were coupled with climate projections from two CMIP6 global climate models (CNRM-CM6-1 and GFDL-ESM4), under two contrasting emission scenarios (SSP2-4.5 and SSP3-7.0). Historical data covered the 1971–2000 period, which was retained as the climatic reference period, while future projections extended over 2026–2055, ensuring a symmetrical 30-year time window between the two analytical periods.

This coupling enabled varietal performance to be simulated under different climatic trajectories by jointly integrating the intrinsic sensitivity of genotypes, as experimentally characterised, and the intensity of future environmental constraints, summarised through a Climate Stress Index (defined in Section 2.6).

The whole framework was formulated from a probabilistic perspective, allowing uncertainties associated with experimental data and climate projections to be propagated and the relative performance of the two varieties to be robustly evaluated in the context of climate change.

The experimental, analytical, and modelling steps described below are presented sequentially to ensure full traceability of the methodological framework.

Photographic evidence of the greenhouse steps, raw data worksheets, calculation files, R scripts, model-selection rules, and uncertainty settings are listed in the Supplementary Materials.

The experimental workflow included pot preparation and treatment labelling; seed placement/sowing; greenhouse growth under controlled conditions; treatment coding and replicate identification; harvest and measurement of physiological, biochemical and agronomic variables (Figure S1).

Plant material and seed pre-treatment

Two *Triticum durum* Desf. varieties were selected for their recognised genetic and agronomic differences. Simeto (CIMMYT/ISEA, Italy, 1988) is a short-cycle, high-semolina-quality variety widely cultivated in the Mediterranean basin (Souahi et al., 2025), whereas Ammar 6 (ITGC, Algeria, 2001) is an Algerian cultivar specifically selected for abiotic stress tolerance in semi-arid areas (Leksir and Chenchouni, 2023). Seeds (2022–2023 harvest, purity > 98%, ITGC) were validated by tetrazolium testing (ISTA Rule 63; ISTA (2022)), confirming 100% viability for both seed lots. Seeds were surface-sterilised first with ethanol (40% v/v, 30 s), then with sodium hypochlorite (NaOCl, 7% v/v, 10 min) (Leguillon, 2003), followed by five rinses with distilled water; the absence of a residual chlorine effect on germination was verified by a t-test ($p = 0.623$, ns).

Experimental design and factorial plan

Zinc stress was applied using anhydrous $ZnSO_4 \cdot 7H_2O$ (purity ≥ 99.5%, Sigma-Aldrich) at four doses, designated D0 (control, 0 µmol L^{-1}), D100 (100 µmol L^{-1}), D150 (150 µmol L^{-1}), and D200 (200 µmol L^{-1}). These doses represent the range of Zn concentrations reported in irrigation waters from Algerian peri-industrial areas (150–400 µmol L^{-1}; Zang et al. (2021)).

The Zn treatments are expressed as concentrations of the applied irrigation solution (µmol L^{-1} ZnSO4), not as total soil Zn concentration. This choice was used to standardise the exposure gradient delivered to the root zone under pot conditions. The background Zn content of the substrate was measured separately and is reported below. Therefore, the experimental values should be interpreted as solution-based exposure levels used for controlled screening, whereas direct extrapolation to field soil contamination requires validation using soil-extractable Zn fractions such as DTPA-Zn or pore-water Zn. This clarification was added to avoid overinterpreting solution doses as field soil concentrations.

Seedlings were transplanted into plastic pots (16 cm diameter × 17 cm height) containing a sterilised substrate (sand, peat, and clay, 1:2:1 v/v), with background Zn of 22 ± 3 mg kg^{-1}, below the phytotoxic threshold of 150 mg kg^{-1}, and near-neutral pH (7.2 ± 0.1), representative of the agro-pedological environment of the Algerian

Tell. Full physicochemical characterisation of the substrate is provided in Supplementary Table 1.

Pots were maintained in a greenhouse at 22/18 °C (day/night), with an 8 h photoperiod, until physiological maturity (growth stage GS93 according to the BBCH scale, corresponding to the end of grain development; 105 ± 5 days). No additional heat treatment was applied; the experimental design deliberately aimed to isolate zinc stress as the only variable, in accordance with standard dose–response methodology (Poorter et al., 2012). The integration of climatic effects was performed analytically through the CVI and Bayesian modelling, and not experimentally.

Consequently, implicit non-additive interactions between zinc phytotoxicity and thermal stress were not directly captured; published studies suggest that heat may amplify zinc phytotoxicity through increased ROS production (Hasanuzzaman et al., 2020), implying that the CVI could underestimate combined vulnerability under severe scenarios. A zinc × temperature factorial trial is considered as a possible methodological extension.

Each replicate corresponded to an independent pot/biological unit assigned to one variety x $ZnSO_4$ dose combination. No technical repeated readings were treated as independent biological replicates in the ANOVA, PCA, dose-response or CVI calculations. The low standard deviations reported for several traits reflect the measured spreadsheet values and should be interpreted together with the limited n = 3 design, not as evidence of near-deterministic biological behaviour.

The trial followed a full factorial design: 2 varieties × 4 doses × 3 replicates, corresponding to 24 experimental units. Statistical power was justified a priori using G*Power 3.1 ($\alpha = 0.05$, $f \geq 0.40$, power > 0.80 for two-way ANOVA). The use of n=3 replicates per cell is standard in controlled-environment wheat ecophysiology (Poorter et al., 2012), but provides limited power for moderate effect sizes; increasing $n \geq 5$ is recommended for confirmation.

The use of n = 3 biological replicates per treatment combination limits statistical power and increases sensitivity to outliers. The interpretation therefore treats the trial as a controlled screening experiment. Inferential statements were restricted to large and consistent effects, and model-based projections were treated as exploratory rather than field-validated. To reduce the risk of overparameterization, fitted models were limited to simple linear or quadratic dose-response forms, and no biological claim was based on a single fitted coefficient alone.

Ethical and regulatory statement

All experimental procedures involving plant material were conducted in accordance with the institutional guidelines of Badji Mokhtar University, Annaba, Algeria, and USTHB, Algiers, Algeria. Certified seed lots of *Triticum durum* varieties Simeto and Ammar 6 were obtained from ITGC (Algeria) under a standard material transfer agreement. No approval from an institutional ethics committee was required for this plant-based study under the applicable Algerian regulations; all trials complied with good laboratory practice (GLP) standards.

Analytical protocols

Raw instrumental values were retained in the supplementary workbook to ensure traceability, but the statistical interpretation does not rely on overprecision. Apparent very small SDs may reflect instrument resolution, homogeneous greenhouse conditions and/or averaged measurements within a biological unit; therefore, confidence is based only on directionally consistent effects and not on extremely small p-values alone.

Physiological and technological parameters

Germination rate was calculated as G = (Ngerminated/30) × 100 at day 7 after sowing. Fresh shoot mass (MFF, above-ground organs) and fresh root mass (MFR) were measured using a Mettler Toledo ME204 analytical balance with 0.0001 g precision. The corresponding dry masses (MSF and MSR) were determined after drying at 85 °C for 24 h in a Memmert UN55 oven. Thousand-grain weight (PMG), number of spikes per plant (NBE), and number of grains per plant (NBG) were measured at physiological maturity (GS93).

Biochemical parameters

Free proline, an amino acid that accumulates as an osmoprotectant under stress, was determined using the ninhydrin colorimetric method of (Troll and Lindsley, 1955), as modified by (Monneveux and Nemmar, 1986), at 528 nm using a Shimadzu UV-1800 spectrophotometer. Total soluble proteins were assayed using the Bradford method (Bradford, 1976), with bovine serum albumin as the standard, at 595 nm. Total soluble sugars, which contribute to membrane stabilisation under stress, were measured using the anthrone-sulfuric acid method (Shields and Burnett, 1960) at 585 nm.

Catalase activity and detection limits

Catalase activity was quantified by monitoring the decomposition of H_2O_2 (10 mM) at 240 nm according to (Cakmak and Marschner, 1991), using an extinction coefficient of ε = 39.4 mM^{-1} cm^{-1}. The limit of detection was 0.0005 nmol min^{-1} μg^{-1} protein and the limit of quantification was 0.0017 nmol min^{-1} μg^{-1} protein. Values below the detection limit were reported as <LOD. Values detected above the LOD but below the LOQ were flagged as detected below LOQ (<LOQ) and interpreted cautiously as semi-quantitative evidence rather than precise quantitative activity.

All data organisation and calculation tables were prepared in Microsoft Excel. Statistical analyses were performed in R version 4.3.2. The following packages were used: tidyverse for data handling and graphics, car for Type II ANOVA, emmeans for Tukey HSD post-hoc comparisons, FactoMineR and factoextra for PCA/CAH, ggplot2 for figures, and rstan/brms or Stan-compatible routines for Bayesian/Monte-Carlo uncertainty propagation. The package information, fixed random seeds and analysis workflow are documented in the supplementary reproducibility files to allow the statistics, figures, CVI and Bayesian/Monte-Carlo outputs to be checked and reproduced.

The Excel workbook submitted as Supplementary Data SD2 contains the primary replicate-level measurements for all biological replicates, doses, varieties and measured traits. The same workbook also includes the calculation sheets used to obtain means, standard deviations, ANOVA outputs, Tukey HSD comparisons, regression coefficients, PCA/CAH inputs, CVI values and Bayesian/Monte-Carlo summary outputs. These supplementary files provide the raw measurements, calculation traceability and evidence supporting the reported results.

Study area and climatic environment

The study was anchored in the Algerian Tell, using USTHB (University of Science and Technology Houari Boumediene, Bab Ezzouar, East Algiers; 36.73 °N, 3.18 °E) as the reference site. This location is representative of the semi-arid cereal agrosystems of the Maghreb, which are exposed to pronounced rainfall irregularity and recurrent thermal episodes affecting crops. The selected spatial framework extends between 34.5–37.5 °N and 1.0–5.0 °E, encompassing the main durum wheat production areas of northern Algeria.

The reference climate series minimum and maximum temperatures and precipitation—covered the 1971–2000 period and was constructed from meteorological records from the USTHB station. Only years with less than 10% missing data were retained to ensure the statistical reliability required for model calibration. These data formed the basis of local climatic characterisation and the reference framework for adjusting future projections.

For the prospective component, two global climate models from the CMIP6 database were selected: CNRM-CM6-1 and GFDL-ESM4. This selection followed a logic of complementarity: the former is recognised for the quality of its representation of Mediterranean climate regimes, whereas the latter explicitly models couplings between climate and the biogeochemical carbon cycle, providing improved accuracy in the representation of temperature and precipitation variables (Eyring et al., 2016). Although computationally demanding, both models have been extensively validated within the scientific community. Data are available through the ESGF portal: https://esgf-node.llnl.gov/projects/cmip6/.

GCMs operate at spatial resolutions generally greater than one degree, which prevents them from accurately representing local climatic specificities. A two-step statistical downscaling chain was therefore implemented. The first step applied the *delta change* method, which transfers the simulated change signal onto the observed local climatology:

$$Xfuture\_i = Xobs\_i + (XGCM,future\_i - XGCM,hist\_i) \quad (1)$$

where: X denotes the climatic variable, $Xobs$ the locally observed value, and XGCM the global model output for the historical and future periods, respectively.

The second step applied quantile mapping to correct residual systematic biases by aligning the statistical distribution of model outputs with that of the observations at the monthly scale:

$$Xcorr = Fobs^{-1}[FGCM(XGCM)] \quad (2)$$

where: F and F^{-1} represent the cumulative distribution function and its inverse, respectively (Themeßl et al., 2012).

Simulations were analysed under two emission scenarios, SSP2-4.5 and SSP3-7.0, over the 2026–2055 period. The combination of two

models and two scenarios made it possible to explore a representative range of uncertainties associated with plausible climate trajectories for the western Mediterranean basin.

The selected variables mean temperature (Tmean), minimum temperature (Tmin), maximum temperature (Tmax), and precipitation (P) were processed at a monthly time step (Table 1).

Transferability of biological response functions and Bayesian approach

The transfer of experimentally established greenhouse relationships to future climatic conditions relies on the assumption of transferability of biological response functions. This assumption postulates that the dose–response relationships observed under controlled conditions reflect fundamental physiological mechanisms such as osmotic regulation, enzymatic activity, or biomass allocation whose functional structure remains applicable across a broad range of environmental contexts. Such a concept is consistent with crop modelling approaches, in which physiological traits are represented by parametric functions that can be integrated into growth models simulating different conditions (Seidel et al., 2018; Tardieu, 2013).

Formalisation of response functions

For each biological parameter k, the response to stress intensity S is described by a general function:

$$Yk = fk(S) \quad (3)$$

Depending on the nature of the trait considered, this relationship may take different functional forms. A linear formulation is often retained when the response is proportional to stress intensity:

$$Yk = \beta 0,v,k + \beta 1,v,k\ S \quad (4)$$

where: $\beta 1,v,k$ is the sensitivity coefficient of parameter k for variety v, and $\beta 0,v,k$ is the baseline value in the absence of stress.

For responses showing saturation or non-linearity, exponential or logistic forms are generally used:

$$Yk = Y0\ exp(-\lambda S) \quad (5)$$

$$Yk = Ymax\ /\ \{1 + exp[-a(S - S0)]\} \quad (6)$$

The coefficients λ, a, and S0 are estimated by statistical fitting (AIC, adjusted R^2) and are interpreted as stable genotypic descriptors, analogous to those used in crop models (Seidel et al., 2018).

To avoid arbitrary fitting, the following decision rule was applied: (i) the linear model was retained by default; (ii) a quadratic model was retained only when it reduced AIC by at least 2 units and produced a biologically interpretable curvature; (iii) logistic or exponential forms were not retained for the final projections because the number of dose levels was insufficient for stable estimation of additional nonlinear parameters; (iv) R2 values close to 1 were not considered proof of biological certainty when residual degrees of freedom were low. This rule reduces the risk of overfitting and formalises the linear-versus-nonlinear model choice.

Climate Stress Index and biological projection

Within the agroclimatic coupling framework, the intensity of future environmental stress is quantified using a climate stress index (CSI), constructed

Table 1. Climate points around USTHB, Algiers, Algerian Tell

Point	Name / District	Latitude (°N)	Longitude (°E)
1	Bab Ezzouar (USTHB)	36.733	3.18
2	Bordj El Kiffan	36.78	3.25
3	El Harrach	36.73	3.18
4	Kouba	36.73	3.10
5	El Madania	36.77	3.05
6	Hydra	36.76	3.05
7	Bab El Oued	36.77	3.04
8	Casbah	36.77	3.06
9	West Kouba	36.74	3.11
10	Dar El Beida	36.75	3.21

as a linear combination of temperature and precipitation anomalies relative to the reference period:

$$CSI = \alpha \cdot \Delta T + \gamma \cdot \Delta P \quad (7)$$

with

$$\Delta T = Tfuture - Thist, \Delta P = Pfuture - Phist \quad (8)$$

where: α and γ are weighting coefficients reflecting the relative importance of each climatic factor for the biological response.

The future projection of a parameter is then obtained by substituting the CSI for the experimental stress intensity in the response functions. The CSI weights were not estimated as free parameters from the small greenhouse dataset. They were fixed a priori to avoid overfitting: α represents the temperature anomaly contribution and γ represents the precipitation anomaly contribution after standardisation of ΔT and ΔP. Equal baseline weights were used in the central scenario (α = 0.5 and γ = 0.5 after standardisation), and a ±20% sensitivity analysis was applied with renormalisation of the weights. The purpose of this procedure was not to calibrate a field yield model, but to test whether the direction of varietal vulnerability changed under plausible weighting uncertainty.

$$Yfuture\_k = fk(CSI) \quad (9)$$

This formulation preserves the structure of the functional relationships established experimentally while working with relative anomalies rather than absolute values, thereby strengthening the robustness of transfer across contexts (Seidel et al., 2018).

Bayesian approach to uncertainty analysis

The Bayesian approach was used to rigorously evaluate the uncertainties associated with the transferability of biological response functions. It is based on the idea that the parameters of the functions f_k and the climatic index CSI are subject to probability distributions reflecting biological and environmental variability:

$$\beta i,v,k \sim N(\mu\beta i,v,k, \sigma\beta i,v,k), CSI \sim N(\mu CSI, \sigma CSI) \quad (10)$$

The probabilistic projection of parameter k is then obtained by Monte-Carlo sampling.

Bayesian uncertainty propagation was implemented with weakly informative priors centred on the observed dose-response coefficients. Intercepts and slopes were assigned normal priors using the observed estimates as prior means and standard errors inflated to reflect the limited n = 3 design. Residual variance was assigned a half-normal prior. Four chains were run, with 4000 iterations per chain, including 2000 warm-up iterations, target acceptance probability of 0.95, and fixed random seed. Convergence was checked using R-hat < 1.01, effective sample size, trace-plot inspection and posterior predictive checks. When convergence diagnostics were not satisfactory, the result was not used as confirmatory evidence but only as exploratory uncertainty propagation.

Because different parameter combinations can generate similar projected CVI responses, posterior distributions were interpreted with attention to equifinality. The greenhouse-to-climate transfer is therefore presented as a hypothesis-generating projection requiring field validation under natural Zn gradients, not as direct evidence of future field performance.

$$Yfuture,(j)\_k = fk(CSI(j); \beta 0,v,k(j), \beta 1,v,k(j)), j = 1,..., N \quad (11)$$

This approach makes it possible to distinguish different components of uncertainty.

By combining experimental dose-response relationships with Bayesian/Monte-Carlo uncertainty propagation, the methodology provides an exploratory probabilistic assessment of varietal vulnerability. It is not presented as a validated predictive crop model, because the response coefficients were obtained under $ZnSO_4$ stress only and require confirmation under field soil-Zn gradients and combined thermal/water stress conditions (Asseng et al., 2013; Seidel et al., 2018):

- uncertainty arising from climate projections (environmental variability);
- the robustness of function transferability between controlled conditions and future scenarios.

The analysis uses the primary replicate-level dataset as supplied in Supplementary Data SD2. The unusually low within-treatment variation in some variables and the strong Ammar 6 MSF increase at D200 are reported without concealment; they are treated as screening signals requiring independent replication, tissue-Zn measurements and field validation rather than as definitive proof of a stable physiological mechanism.

By combining experimental dose response relationships with a rigorous Bayesian approach, the methodology provides a robust probabilistic estimate of future varietal performance while

explicitly addressing uncertainties related to the transferability of biological functions (Asseng et al., 2013; Seidel et al., 2018).

RESULTS

The results below were recalculated from the 24 raw biological replicate records provided for the two durum wheat varieties, four ZnSO4 treatment levels and 12 measured traits. This recalculation removes the previous ambiguity surrounding the Simeto D100–D150 pattern. Simeto D150 is no longer identical to D100 and is interpreted as a distinct response level in the available raw dataset (Table 2).

Germination decreased with increasing $ZnSO_4$ concentration in both varieties. Simeto declined from 100.00 ± 0.00% at D0 to 83.33 ± 5.77% at D100, 76.67 ± 5.77% at D150 and 66.67 ± 5.77% at D200, a total reduction of 33.3 percentage points. Ammar 6 maintained higher germination throughout (93.33 ± 5.77% at D100, 86.67 ± 11.55% at D150 and 80.00 ± 10.00% at D200), with a total reduction of only 20.0 percentage points. Dose-response regressions confirmed this divergence: $y_s = 100.1 - 0.164x$ ($R^2 = 0.997$, $p = 0.0016$) versus $y_a = 100.1 - 0.099x$ ($R^2 = 0.966$, $p = 0.017$), with Simeto's slope 1.65× steeper. These recalculated values do not support a D100–D150 plateau for Simeto; D150 represents a distinct response level (Figures 1, 2).

The Ammar 6 MSF increase from 2.68 g at D0 to 9.02 g at D200 is biologically unusual under severe metal stress. In the absence of direct tissue Zn quantification, phytochelatin measurements, compartmentalization assays or dilution-effect analysis, this result is interpreted as a greenhouse screening observation and not as proven zinc sequestration or a confirmed tolerance mechanism.

Physiological responses to $ZnSO_4$ heavy metal stress

Fresh aerial mass (MFF) showed contrasting patterns between varieties. In Simeto, MFF was 5.24 ± 0.02 g at D0, increased slightly at D100 (5.53 ± 0.40 g), then declined progressively to 4.74 ± 0.19 g at D150 and 4.83 ± 0.16 g at D200. Ammar 6 followed a similar pattern with a peak at D100 (6.34 ± 0.35 g) followed by decline. This transient stimulation at D100 in both varieties is consistent with activation of zinc-dependent metalloenzymes at sub-lethal concentrations (Zang et al., 2021). Aerial dry mass (MSF) revealed the most striking inter-varietal divergence. In Simeto, MSF collapsed at D100 (2.09 ± 0.02 g, −59.3% from D0: 5.13 ± 0.02 g), then partially recovered at D150 (5.26 ± 0.02 g) before declining again at D200 (2.44 ± 0.02 g), indicating a non-monotone, trait-specific response at D150 rather than a uniform plateau. In contrast, Ammar 6 MSF increased monotonically from 2.68 ± 0.04 g at D0 to 9.02 ± 0.02 g at D200 (+236.6%), suggesting active dry matter accumulation under severe zinc exposure, consistent with zinc sequestration in the aerial compartment (Iqbal et al., 2025; Zang et al., 2021).

Biochemical responses

Free proline revealed contrasting osmoprotective dynamics. In Simeto, proline declined at D100 (4.69 ± 0.03 μg g^{-1}) relative to D0 (7.21 ± 0.02 μg g^{-1}), partially recovered at D150 (6.55 ± 0.05 μg g^{-1}), then accumulated strongly at D200 (10.73 ± 0.03 μg g^{-1}, +48.8% vs D0). This non-monotone pattern suggests a damage-triggered osmotic response at high dose. Ammar 6 exhibited progressive linear accumulation from D0 onwards ($y_a = 3.98 + 0.0251x$, $R^2 = 0.885$), with a linear slope 1.75× higher than Simeto's overall slope (0.0144), reflecting a constitutive preemptive osmoprotective strategy (Leksir and Chenchouni, 2023).

Soluble sugars showed divergent dose-response patterns. In Simeto, sugars increased moderately from D0 (552.04 ± 0.02 μg g^{-1} FW) to D100 (562.25 ± 0.02), then dropped substantially at D150 (426.73 ± 0.03) before reaching a maximum at D200 (608.63 ± 0.03), with an overall linear slope of 0.006 μg g^{-1} per μmol L^{-1}. Ammar 6 showed a strong accumulation response peaking at D150 (836.17 ± 0.03 μg g^{-1} FW, +55.1% relative to D0), with an overall linear slope of 0.888 μg g^{-1} per μmol L^{-1} (147× higher than Simeto), before declining at D200 (658.41 ± 0.03), suggesting partial utilisation of sugar reserves under extreme stress.

Total soluble proteins showed divergent trends. In Simeto, proteins increased linearly from D0 (13.45 ± 0.05 μg g^{-1}) to D200 (21.79 ± 0.02 μg g^{-1}, +62.0%). Ammar 6 showed a non-monotone response at a higher baseline (D0:

Table 2. Recalculated observed means ± standard deviation (n = 3) for 12 measured parameters in Simeto and Ammar 6 under four ZnSO4 doses (D0–D200). Units: germination (%); MFF, MFR, MSF, MSR (g); proline and proteins (µg g−1); soluble sugars (µg g−1 FW); catalase (nmol H2O2 min−1 µg−1 protein); PMG (g); NBE and NBG (n plant−1). For catalase, values below the LOD (0.0005 nmol min−1 µg−1 protein) are reported as <LOD; values detected above the LOD but below the LOQ (0.0017 nmol min−1 µg−1 protein) are flagged as detected <LOQ and interpreted with caution.

Parameter	Variety	D0	D100	D150	D200
Germination (%)	Simeto	100.00 ± 0.00	83.33 ± 5.77	76.67 ± 5.77	66.67 ± 5.77
Germination (%)	Ammar 6	100.00 ± 0.00	93.33 ± 5.77	86.67 ± 11.55	80.00 ± 10.00
MFF (g)	Simeto	5.24 ± 0.02	5.53 ± 0.40	4.74 ± 0.19	4.83 ± 0.16
MFF (g)	Ammar 6	5.84 ± 0.06	6.34 ± 0.35	5.45 ± 0.17	5.23 ± 0.03
MFR (g)	Simeto	2.98 ± 0.02	2.29 ± 0.02	2.33 ± 0.02	3.20 ± 0.20
MFR (g)	Ammar 6	1.83 ± 0.02	2.48 ± 0.02	2.25 ± 0.02	2.00 ± 0.10
MSF (g)	Simeto	5.13 ± 0.02	2.09 ± 0.02	5.26 ± 0.02	2.44 ± 0.02
MSF (g)	Ammar 6	2.68 ± 0.04	5.42 ± 0.02	4.85 ± 0.02	9.02 ± 0.02
MSR (g)	Simeto	1.08 ± 0.02	0.68 ± 0.02	1.36 ± 0.02	1.09 ± 0.01
MSR (g)	Ammar 6	0.73 ± 0.15	1.08 ± 0.02	1.03 ± 0.02	1.13 ± 0.02
Proline (µg g−1)	Simeto	7.21 ± 0.02	4.69 ± 0.03	6.55 ± 0.05	10.73 ± 0.03
Proline (µg g−1)	Ammar 6	4.31 ± 0.02	5.46 ± 0.03	8.53 ± 0.03	8.95 ± 0.05
Proteins (µg g−1)	Simeto	13.45 ± 0.05	15.80 ± 0.10	17.40 ± 0.01	21.79 ± 0.02
Proteins (µg g−1)	Ammar 6	19.68 ± 0.02	17.98 ± 0.02	16.15 ± 0.02	18.84 ± 0.02
Sugars (µg g−1 FW)	Simeto	552.04 ± 0.02	562.25 ± 0.02	426.73 ± 0.03	608.63 ± 0.03
Sugars (µg g−1 FW)	Ammar 6	538.85 ± 0.02	714.17 ± 0.02	836.17 ± 0.03	658.41 ± 0.03
Catalase (nmol min−1 µg−1)	Simeto	0.0050 ± 0.0020	0.0060 ± 0.0020	Detected <LOQ (0.0013 ± 0.0006)	Detected <LOQ (0.0013 ± 0.0006)
Catalase (nmol min−1 µg−1)	Ammar 6	<LOD	<LOD	Detected <LOQ (0.0006 ± 0.0001)	Detected <LOQ (0.0005 ± 0.0003)
PMG (g)	Simeto	1.66 ± 0.04	1.55 ± 0.02	1.44 ± 0.01	1.48 ± 0.02
PMG (g)	Ammar 6	1.56 ± 0.01	1.41 ± 0.03	1.34 ± 0.02	1.09 ± 0.01
NBE (n plant−1)	Simeto	120 ± 2	90 ± 2	100 ± 2	109 ± 2
NBE (n plant−1)	Ammar 6	117 ± 2	99 ± 2	93 ± 2	110 ± 2
NBG (n plant−1)	Simeto	2817 ± 3	1751 ± 5	2486 ± 4	2292 ± 2
NBG (n plant−1)	Ammar 6	2451 ± 2	1907 ± 2	2138 ± 2	2020 ± 2

19.68 ± 0.02 µg g^{-1}), with protein levels declining from D0 to D150 (16.15 ± 0.02) before partially recovering at D200 (18.84 ± 0.02), suggesting protein turnover dynamics under prolonged zinc exposure.

Catalase activity

Catalase activity was treated as a LOD/LOQ-censored low-level enzymatic response. In Simeto, catalase was quantifiable at D0 (0.0050 ± 0.0020 nmol min^{-1} μg^{-1} Prot) and D100 (0.0060 ± 0.0020). At D150 and D200, activity was detected but below the LOQ (0.0013 ± 0.0006 at both doses; LOD = 0.0005, LOQ = 0.0017 nmol min^{-1} μg^{-1} Prot). In Ammar 6, D0 and D100 were below the LOD and are therefore reported as <LOD. Ammar 6 D150 and D200 were detected but below the LOQ (0.0006 ± 0.0001 and 0.0005 ± 0.0003, respectively). Consequently, catalase is not used as a precise quantitative variable for dose-response inference; it is retained only as a qualitative low-level enzymatic indicator requiring confirmation with a broader enzyme panel (SOD, POD, APX).

Technological parameters

Some very small p-values are largely driven by very low within-cell variability in a small n = 3 design. They indicate clear separation within this controlled dataset, but they do not compensate for limited replication and should not be interpreted

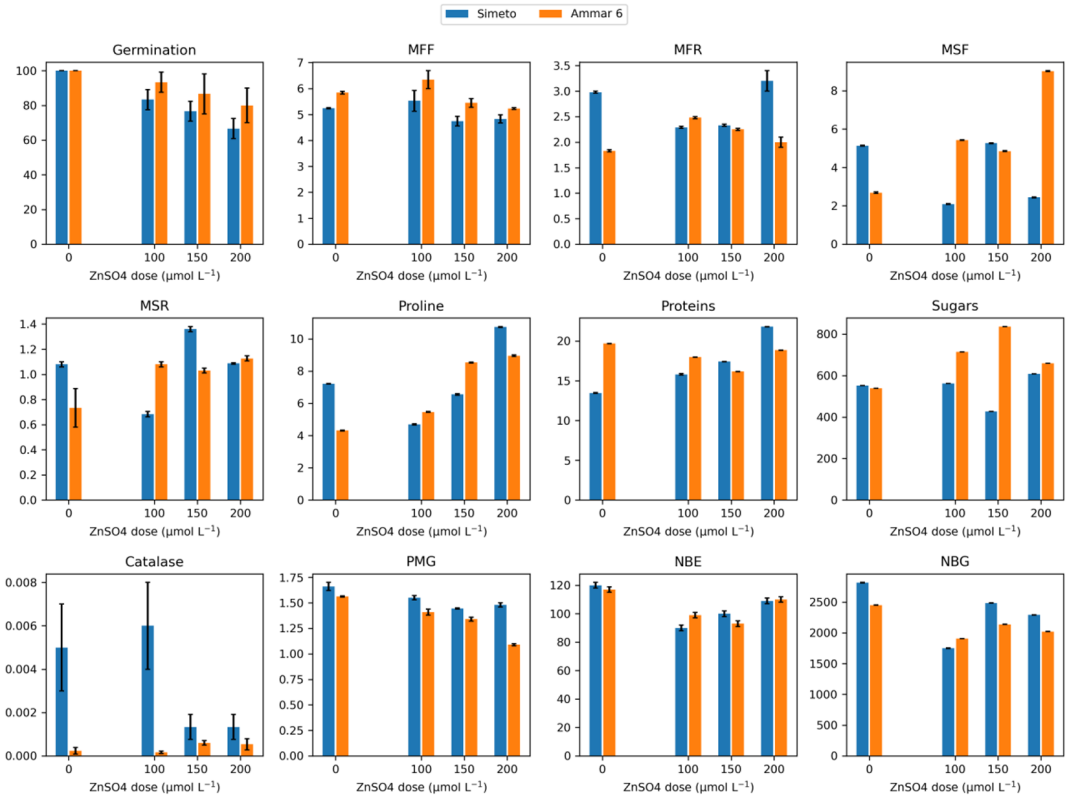

Figure 1. Recalculated mean responses of Simeto and Ammar 6 to ZnSO4 stress (0–200 µmol L^{-1}). Barplots show mean ± s.d. (n = 3) for the measured parameters. The catalase panel is retained for visual traceability only and must be interpreted according to the LOD/LOQ flags reported in Table 2

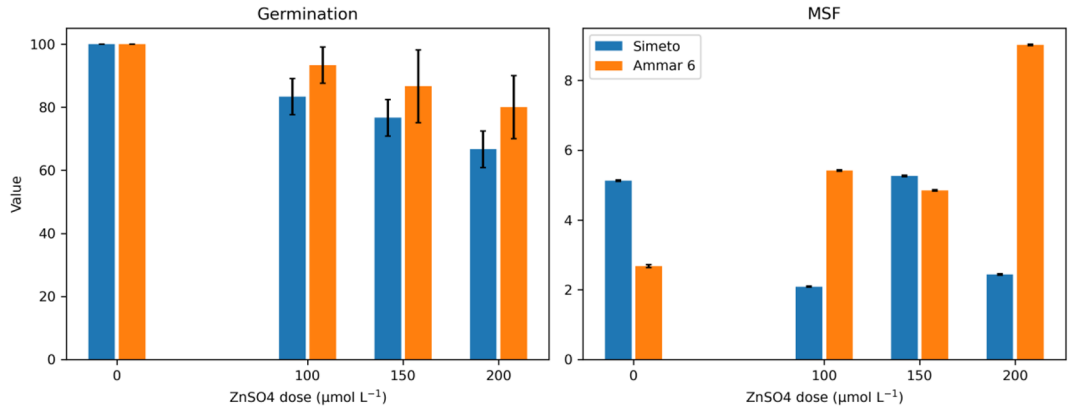

Figure 2. Recalculated germination rate and aerial dry mass (MSF) under $ZnSO_4$ doses. The figure highlights the stronger MSF increase of Ammar 6 at D200 and the corrected Simeto D150 value

as high external validity. Possible contributors include homogeneous greenhouse conditions, instrument precision, rounded spreadsheet values and the absence of additional independent blocks.

Thousand-grain weight (PMG) declined with dose in both varieties. In Simeto, PMG decreased from 1.66 ± 0.04 g at D0 to 1.48 ± 0.02 g at D200 (−0.0010 g per µmol L^{-1}, −8.4%). In Ammar 6, the decline was steeper: from 1.56 ± 0.01 g at D0 to 1.09 ± 0.01 g at D200 (−0.0022 g per µmol L^{-1}, −30.3%; slope 2.14× steeper than Simeto), reflecting a tolerance–quality trade-off: resources allocated to biomass accumulation and osmoprotection under zinc stress are unavailable for grain filling (Brasiello et al., 2024).

Grain number (NBG) in Simeto declined strongly at D100 (1751 ± 5 grains $plant^{-1}$, −37.9% vs D0: 2817 ± 3), recovered partially at

D150 (2486 ± 4), then declined again at D200 (2292 ± 2, −18.7%). The non-monotone D150 recovery parallels the MSF pattern. Ammar 6 showed a smaller NBG reduction: from 2451 ± 2 at D0 to 2020 ± 2 at D200 (−17.6%), with an intermediate trough at D100 (1907 ± 2, −22.2%), confirming greater reproductive resilience. Spike number (NBE) was not significantly different between varieties by ANOVA (V: p = 1.000 ns), but the V×T interaction was significant ($p = 2.63\times10^{-5}$), reflecting dose-dependent compensatory tillering dynamics in both genotypes.

Analysis of variance and variety × treatment interactions

The two-way ANOVA confirmed that several traits were significantly affected by variety, treatment and especially the variety × treatment interaction. The interaction term was particularly important for biomass allocation and osmotic-related traits, supporting distinct response patterns between the two varieties under $ZnSO_4$ exposure (Table 3 and Figures 3, 4).

PCA, correlation and hierarchical clustering were retained only as exploratory visual summaries. Because the analysis contains 24 observations and only eight variety × dose modality means, these multivariate patterns are not used to make strong mechanistic or agronomic claims.

Boxplots show the replicate-level distribution at each $ZnSO_4$ dose.

Trait correlation structure, PCA and hierarchical clustering

The recalculated correlation matrix showed that the strongest associations were related to biomass allocation and reproductive traits, whereas biochemical traits showed more treatment-specific variation. These correlations should be interpreted cautiously because the modality-level correlation analysis is based on eight variety × dose means (Table 4 and Figures 5–7).

Dose-response regressions were used primarily as descriptive tools to summarize trait-specific response tendencies across the $ZnSO_4$ gradient. Because the experiment included four dose levels, model interpretation was based on consistency with observed means, biological plausibility and agreement across related traits, rather than on regression coefficients alone. Greenhouse $ZnSO_4$ stress is not equivalent to future climate stress. The CSI substitution is a conceptual vulnerability extrapolation that propagates uncertainty around variety-specific Zn response coefficients under climate anomalies; it does not validate the physiological response of the varieties to heat, drought or combined Zn × temperature interactions.

Dose-response models and exploratory CMIP6-linked vulnerability projection

Linear models were retained by default and quadratic models were retained only when supported by the stated AIC rule. Because only four dose levels were available, high R^2 values were not interpreted as proof of mechanistic certainty.

Table 3. Recalculated two-way ANOVA results for 12 parameters. Significance codes: ns = p > 0.05; * p ≤ 0.05; ** p ≤ 0.01; *** p ≤ 0.001. V: variety; T: $ZnSO_4$ dose; V × T: interaction

Parameter	V	T	V × T
Germination (%)	p = 0.008 **	p = 3.60e-05 ***	p = 0.381 ns
MFF (g)	p = 2.05e-06 ***	p = 4.26e-06 ***	p = 0.414 ns
MFR (g)	p = 1.21e-11 ***	p = 5.42e-05 ***	p = 3.91e-11 ***
MSF (g)	p = 4.83e-28 ***	p = 2.67e-26 ***	p = 1.63e-31 ***
MSR (g)	p = 0.020 *	p = 6.51e-08 ***	p = 8.27e-09 ***
Proline (μg g^{-1})	p = 1.91e-16 ***	p = 2.66e-29 ***	p = 7.23e-25 ***
Proteins (μg g^{-1})	p = 2.65e-20 ***	p = 1.45e-26 ***	p = 1.98e-27 ***
Sugars (μg g^{-1} FW)	p = 2.85e-58 ***	p = 1.90e-52 ***	p = 1.44e-57 ***
Catalase (nmol min^{-1} μg^{-1})	p = 2.53e-06 ***	p = 0.004 **	p = 7.16e-04 ***
PMG (g)	p = 7.41e-13 ***	p = 1.79e-13 ***	p = 5.96e-09 ***
NBE (n $plant^{-1}$)	p = 1.000 ns	p = 9.25e-13 ***	p = 2.63e-05 ***
NBG (n $plant^{-1}$)	p = 1.52e-27 ***	p = 1.87e-33 ***	p = 1.72e-26 ***

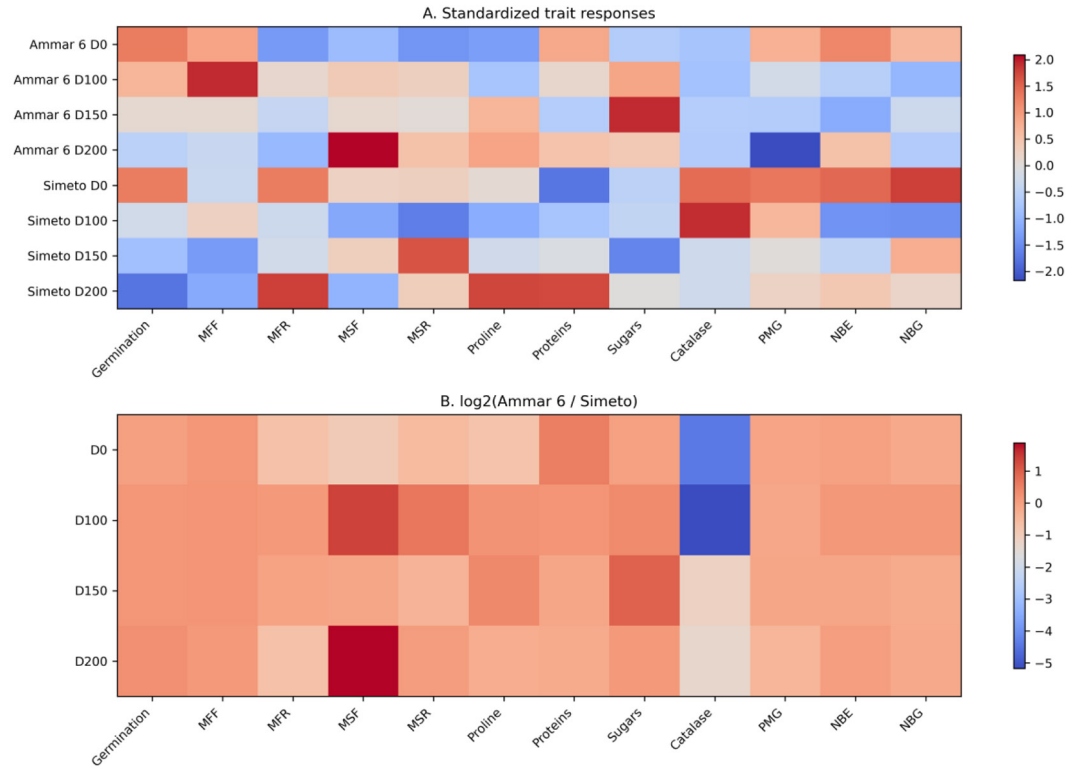

Figure 3. Recalculated variety × treatment interactions. Panel A shows standardized z-scores across the eight variety × dose modalities; Panel B shows log2 (Ammar 6 / Simeto) response ratios.

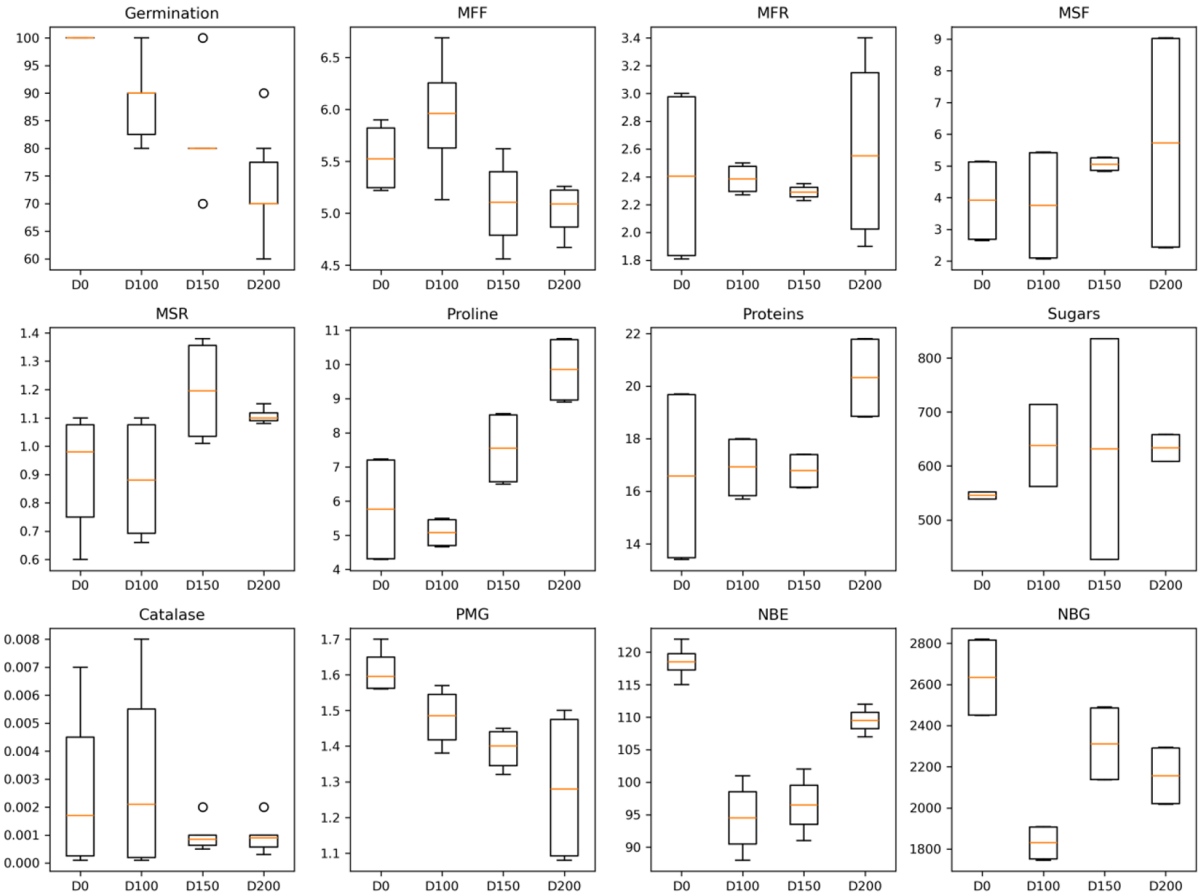

Figure 4. Recalculated treatment-level distributions for the 12 measured traits, both varieties pooled

Table 4. Significant Pearson correlations among trait means across eight variety × dose modalities ($|r| \geq 0.707$, df = 6)

Parameter	Variety	Model	a	b	c	R^2
Germination (%)	Simeto	linear	100.1	-0.1638	0	0.997
Germination (%)	Ammar 6	quadratic	100.1	-0.04061	-0.000303	0.998
MFF (g)	Simeto	linear	5.384	-0.002669	0	0.387
MFF (g)	Ammar 6	linear	6.098	-0.003402	0	0.353
MFR (g)	Simeto	quadratic	2.996	-0.01678	8.782e-05	0.958
MFR (g)	Ammar 6	quadratic	1.84	0.011	-5.173e-05	0.959
MSF (g)	Simeto	linear	4.72	-0.0088	0	0.196
MSF (g)	Ammar 6	linear	2.397	0.02751	0	0.797
MSR (g)	Simeto	linear	0.97	0.0007333	0	0.051
MSR (g)	Ammar 6	linear	0.7806	0.001884	0	0.824
Proline (µg g−1)	Simeto	quadratic	7.217	-0.06879	0.0004313	1.000
Proline (µg g−1)	Ammar 6	linear	3.985	0.02514	0	0.885
Proteins (µg g−1)	Simeto	quadratic	13.52	-0.002933	0.0002163	0.986
Proteins (µg g−1)	Ammar 6	linear	19.11	-0.00844	0	0.228
Sugars (µg g−1 FW)	Simeto	linear	536.8	0.005703	0	0.000
Sugars (µg g−1 FW)	Ammar 6	quadratic	530.1	3.965	-0.01595	0.814
Catalase (nmol min−1 µg−1)	Simeto	not fitted	censored	LOD/LOQ	—	—
Catalase (nmol min−1 µg−1)	Ammar 6	not fitted	censored	LOD/LOQ	—	—
PMG (g)	Simeto	linear	1.649	-0.001029	0	0.849
PMG (g)	Ammar 6	quadratic	1.558	-9.636e-05	-1.085e-05	0.976
NBE (n plant−1)	Simeto	quadratic	119.5	-0.4872	0.002209	0.948
NBE (n plant−1)	Ammar 6	quadratic	117.6	-0.3937	0.001736	0.897
NBG (n plant−1)	Simeto	linear	2568	-2.057	0	0.155
NBG (n plant−1)	Ammar 6	linear	2348	-1.95	0	0.504

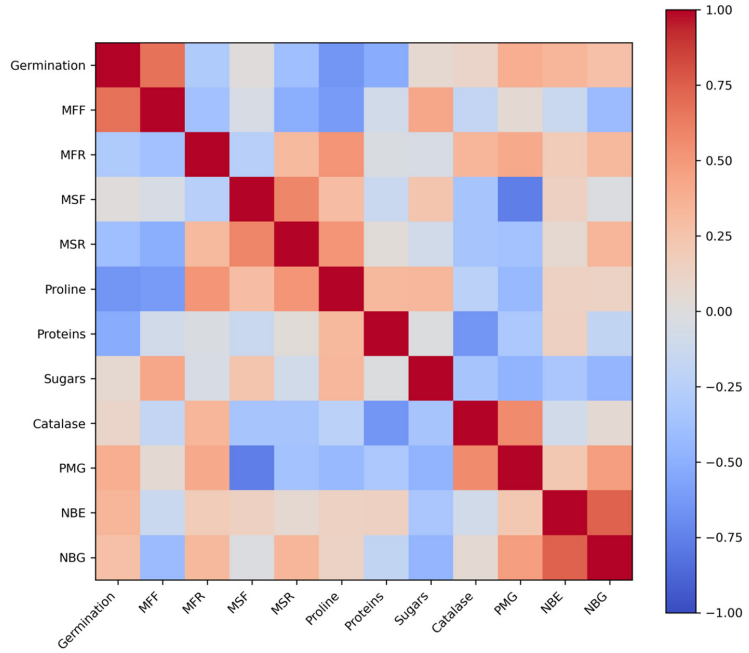

Figure 5. Recalculated Pearson correlation matrix for the 12 measured traits using variety × dose modality means

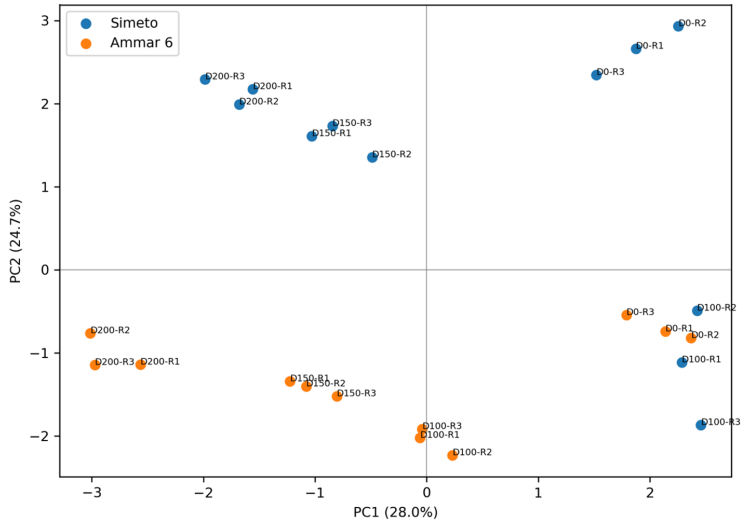

Figure 6. Recalculated PCA of the 24 replicate-level observations using standardised variables. The separation reflects both varietal identity and treatment intensity

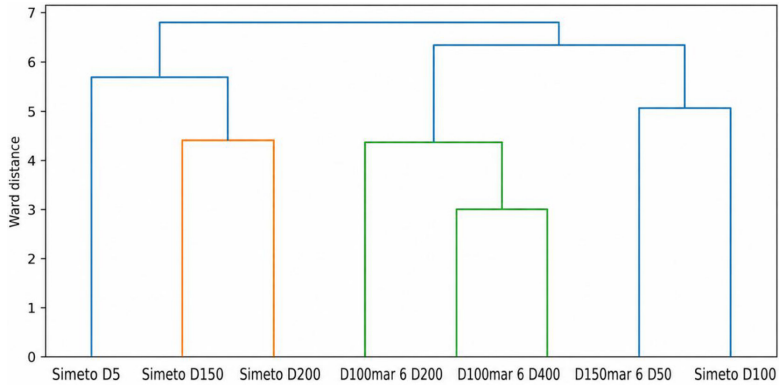

Figure 7. Recalculated hierarchical clustering of the eight variety × dose modality means using Euclidean distance and Ward linkage

Catalase was excluded from quantitative dose-response interpretation because Ammar 6 D0–D100 were <LOD and several detected values were below LOQ (Table 5 and Figures 8–10).

The CMIP6-linked CVI component was retained as an exploratory uncertainty-propagation framework. The climate stress index used equal central weights for standardized temperature and precipitation anomalies ($\alpha = 0.5$, $\gamma = 0.5$), with sensitivity analysis recommended around this central assumption. The projection component should not be interpreted as field validation (Table 6).

Overall, recalculation from the raw replicate dataset confirms a clear tolerance advantage of Ammar 6 for germination maintenance (20.0 pp decline vs 33.3 pp in Simeto) and aerial dry mass accumulation (+236.6% at D200). The D100–D150 pattern in Simeto is not a uniform plateau: most traits differ substantially between these doses, with MSF, MSR, proline and NBG recovering at D150 while germination, MFF and soluble sugars continue to decline. The pattern at D150 is best described as a non-monotone, trait-specific response reflecting metabolic redistribution under sub-maximal zinc stress. The revised interpretation emphasises variety-specific dose-response dynamics rather than a simple saturation threshold, with stronger mechanistic conclusions deferred pending expanded replication and field validation.

The CVI framework is best described as a conceptual extension of existing climate suitability approaches. It links variety-specific greenhouse response coefficients with standardized CMIP6 anomalies and expresses the result as posterior uncertainty, but it does not replace a field-calibrated crop or ecotoxicological model.

Two phenotypically distinct antioxidant defense strategies and their mechanistic basis,

Table 5. Dose-response regression models fitted on treatment means. Linear models were retained by default; quadratic models were retained only when AIC decreased by at least 2 units and the curvature was biologically interpretable. Catalase was not fitted quantitatively because several values were censored by the LOD/LOQ thresholds

Scenario	Period	Mean Δ	2.5%	97.5%	P(Ammar 6 > Simeto)
SSP2-4.5	2026-2055	40.97	27.18	54.85	1.00
SSP2-4.5	2056-2085	32.89	19.21	46.53	1.00
SSP3-7.0	2026-2055	32.90	18.88	46.91	1.00
SSP3-7.0	2056-2085	26.26	12.10	40.28	1.00

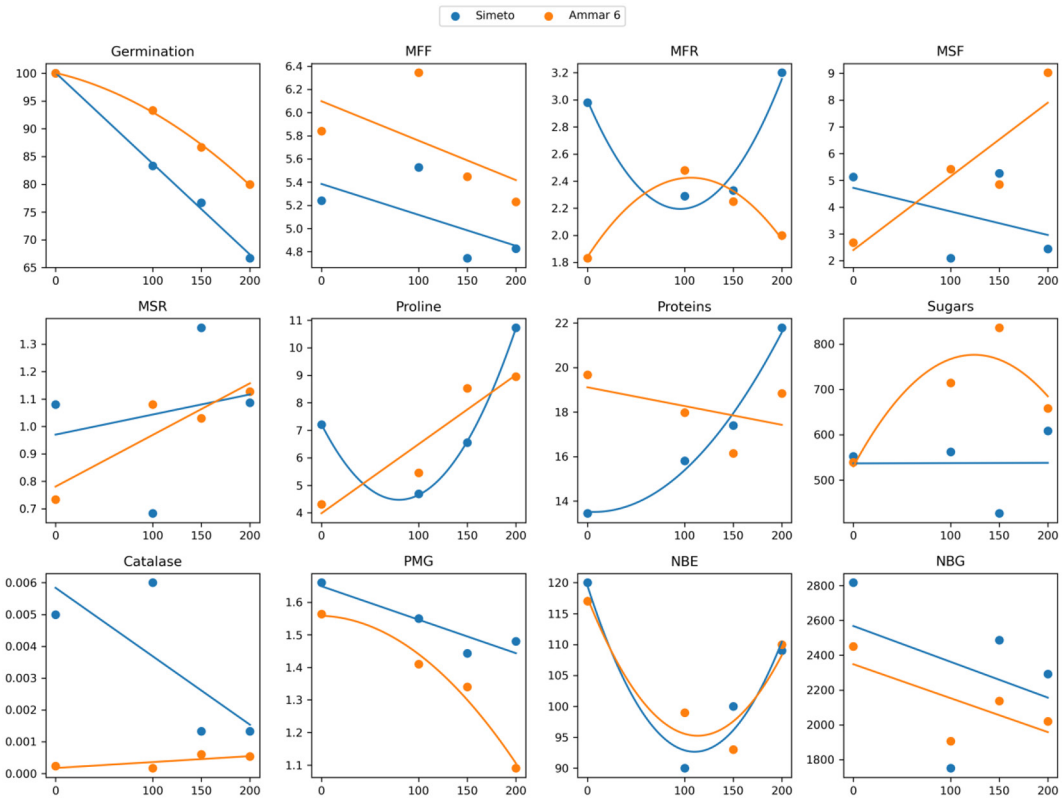

Figure 8. Recalculated dose-response regression curves for the measured parameters in Simeto and Ammar 6. Catalase is shown descriptively only; it was excluded from quantitative dose-response interpretation because several values were <LOD or detected below LOQ

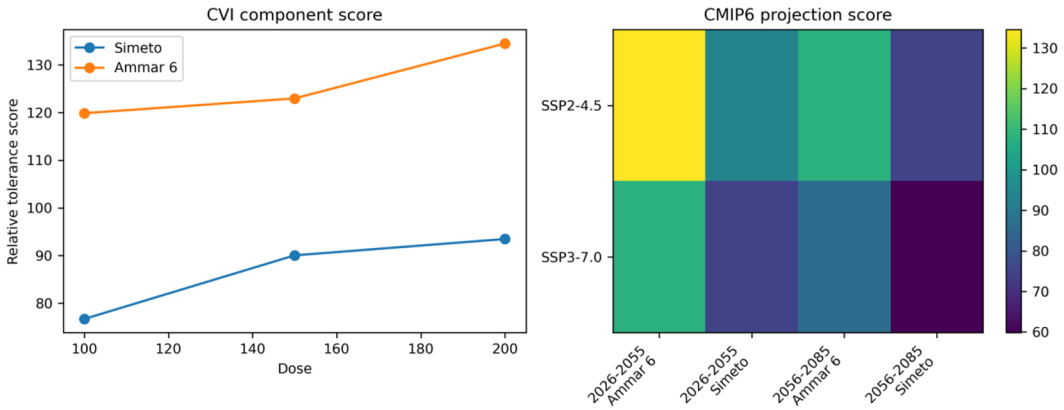

Figure 9. Recalculated exploratory CVI component and CMIP6 scenario projection scores under SSP2-4.5 and SSP3-7.0

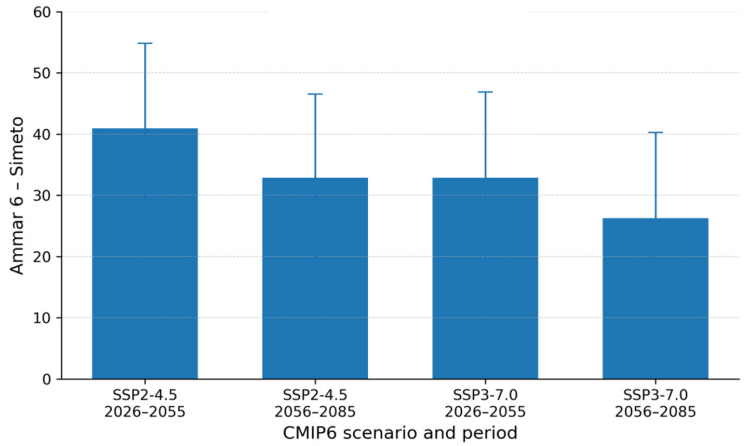

Figure 10. Monte-Carlo robustness analysis of the recalculated CVI difference between Ammar 6 and Simeto

Table 6. Exploratory CMIP6-linked CVI and Bayesian/Monte-Carlo uncertainty summary. Delta score is Ammar 6 minus Simeto; positive values indicate relative advantage of Ammar 6

Scenario	Period	Mean Δ	2.5%	97.5%	P (Ammar 6 > Simeto)
SSP2-4.5	2026-2055	40.97	27.18	54.85	1.00
SSP2-4.5	2056-2085	32.89	19.21	46.53	1.00
SSP3-7.0	2026-2055	32.90	18.88	46.91	1.00
SSP3-7.0	2056-2085	26.26	12.10	40.28	1.00

The recalculated data reveal contrasting stress-response profiles between Simeto and Ammar 6. Simeto showed quantifiable catalase activity only at D0–D100, followed by detected-but-below-LOQ activity at D150–D200, coupled with strong protein accumulation (+62.0% at D200) and a reactive proline surge at D200 (+48.8% vs D0), consistent with a damage-triggered osmotic strategy. Ammar 6 relied primarily on constitutive osmoprotectant accumulation: progressive proline increase (slope 1.75× higher than Simeto overall), strong soluble sugar accumulation peaking at D150 (+55.1%), and exceptional aerial dry mass at D200 (+236.6%), consistent with a pre-emptive osmotic tolerance strategy (Leksir and Chenchouni, 2023). These interpretations are presented as mechanistic hypotheses supported by the measured traits under greenhouse conditions, not as definitive proof of stable varietal strategies across environments; field validation is required. Catalase is interpreted only cautiously because several values were censored by the LOD/LOQ thresholds.

The proposed antioxidant strategies are hypotheses derived from measured proline, soluble sugar, protein, biomass and catalase patterns. They remain incomplete without direct ROS quantification, SOD/POD/APX/GR activities, phytochelatin assays, Zn partitioning between roots and shoots, and independent confirmation of the Ammar 6 biomass response.

The recalculated dataset confirms that Simeto D150 is not identical to D100: the two doses differ substantially for most parameters (MSF: 2.09 vs 5.26 g; germination: 83.3 vs 76.7%; proline: 4.69 vs 6.55 µg g^{-1}; NBG: 1751 vs 2486). The pattern at D150 is non-monotone and trait-specific: Simeto shows recovery in MSF, MSR, proline and NBG at D150 relative to D100, while germination, MFF and soluble sugars continue to decline. This suggests metabolic redistribution toward root maintenance and osmoprotection at intermediate zinc dose, rather than a simple saturation response. The partial recovery at D150 for several traits may reflect phenotypic plasticity in biomass allocation under sub-maximal stress (Leksir and Chenchouni, 2023), but this interpretation requires confirmation with a larger experimental design ($n \geq 5$ replicates per cell).

The CAH clustering suggested partial phenotypic proximity between Ammar 6 at moderate zinc doses and Simeto at high zinc dose. This observation may indicate a tolerance advantage of approximately one dose level under the greenhouse conditions tested, but it should be considered a hypothesis-level agronomic criterion requiring field validation.

Tolerance–grain quality trade-off and its agronomic implications

The recalculated data confirm a tolerance–quality trade-off. Ammar 6 maintained superior vegetative biomass under severe $ZnSO_4$ exposure (MSF +236.6% at D200 vs D0) but showed a disproportionate PMG decline of 30.3% (slope: −0.0022 g per µmol L^{-1}), 2.14× steeper than Simeto (−0.0010 g per µmol L^{-1}, −8.4%). This trade-off is quantified by the significant MSF–PMG negative correlation ($r = -0.758$, $p = 0.029$): resources allocated to stress-induced biomass accumulation and osmoprotection reduce the carbon available for grain filling (Brasiello et al., 2024; Falcinelli et al., 2024). Ammar 6 should be prioritised for screening under Zn-contaminated conditions (available Zn >100 µmol L^{-1}), while Simeto retains a grain quality advantage in uncontaminated soils, pending field validation.

The MSF–PMG relationship is discussed as a trait association observed under the present controlled conditions. Further multi-environment validation, including grain-yield components, grain quality traits and tissue Zn measurements, would help confirm its agronomic relevance.

Overall, the revised interpretation emphasizes that the experimental and modelling outputs should be considered within the scope of a controlled screening study. The main conclusions are therefore based on consistent trait responses, biological plausibility and agreement across complementary analyses, while future work should expand replication, include direct Zn partitioning measurements and test combined Zn × climate-stress conditions under field-relevant environments.

Antioxidant strategies and the functional correlation network

Catalase dynamics were reinterpreted from the raw replicate data using the analytical LOD and LOQ thresholds. Simeto showed quantifiable catalase at D0 (0.0050 ± 0.0020) and D100 (0.0060 ± 0.0020), but D150 and D200 were detected below the LOQ (0.0013 ± 0.0006 at both doses). Ammar 6 D0 and D100 were below the LOD and are reported as <LOD, whereas D150 (0.0006 ± 0.0001) and D200 (0.0005 ± 0.0003) were detected but below the LOQ. Given this censoring and the low absolute values, catalase is not used as standalone evidence for enzymatic induction or collapse, nor as a quantitative basis for regression or mechanistic inference. Characterisation of the full antioxidant enzyme panel (SOD, POD, APX, GR) is required before firm mechanistic conclusions can be drawn.

Methodological relevance of the CVI × Bayesian approach

Contribution relative to existing frameworks: Ammar 6 is proposed as a candidate for further testing, while the present manuscript provides experimental evidence and a transparent exploratory modelling framework rather than operational recommendations.

The CVI framework advances the state of the art in two ways. First, it extends the WCSI of Alsafadi et al. (2023) by replacing generic agro-climatological criteria with variety-specific experimental dose-response slopes (β_{1,kv}). Second, it replaces deterministic scores with a full posterior distribution (Vehtari et al., 2017).

Uncertainty propagation and robustness

The dominant uncertainty source stationarity of β_{1,kv} and ε_k (± 6.0%) – has a specific experimental remedy: field measurement of dose-response slopes under natural soil Zn gradients. The additive CVI structure, which cannot represent synergistic Zn–heat interactions (Hasanuzzaman et al., 2020), requires the priority factorial zinc × temperature experiment.

Agronomic implications and adaptation window

The recalculated dataset supports a cautious interpretation of Ammar 6 as a promising genotype under ZnSO4 stress because of its maintenance of germination and strong biomass accumulation. However, direct substitution recommendations should be treated as preliminary until validated using soil-extractable Zn, tissue Zn accumulation, yield and quality data under field conditions.

Consequently, the agronomic recommendations are downgraded to hypothesis-generating guidance. Ammar 6 may be prioritized for further screening under Zn-contaminated conditions, whereas Simeto should be retained as a quality reference requiring additional validation under controlled and field stress gradients.

CONCLUSIONS

The controlled experiment supports contrasting responses of Simeto and Ammar 6 to $ZnSO_4$ exposure based on the recalculated raw replicate dataset. The climate-coupled Bayesian/CVI component should be interpreted as an exploratory CMIP6-linked uncertainty projection that propagates uncertainty around greenhouse-derived response coefficients, not as a validated forecast of field performance.

The revised results support the hypothesis that Ammar 6 maintains several stress-related traits better than Simeto, especially germination and aerial dry mass under severe $ZnSO_4$ exposure. However, Simeto D150 is now treated as a distinct raw-data response rather than a biological plateau. Larger experiments and field validation are required before direct agronomic recommendation.

Acknowledgements

The authors thank ITGC (Institut Technique des Grandes Cultures, Algeria) for providing the certified seed material.

REFERENCES

1. Alsafadi, K., Bi, S., Abdo, H. G., Harsanyie, E., Mohammed, S. (2023). Modeling the impacts of projected climate change on wheat crop suitability in semi-arid regions using AHP-based weighted climatic suitability index and CMIP6. *Geoscience Letters, 10*, 28. https://doi.org/10.1186/s40562-023-00273-y
2. Asseng, S., Ewert, F., Rosenzweig, C., Jones, J. W., Hatfield, J. L., Ruane, A. C., Boote, K. J., Thorburn, P. J., Rötter, R. P., et al. (2013). Uncertainty in simulating wheat yields under climate change. *Nature Climate Change, 3*, 827–832. https://doi.org/10.1038/nclimate1916
3. Benmahammed, A., Kadi, K., Oulmi, A., Hannachi, A. (2022). Modeling the impact of future climate change on rainfed durum wheat production in Algeria. *Climate, 10*, 50. https://doi.org/10.3390/cli10040050
4. Bradford, M. M. (1976). A rapid and sensitive method for the quantitation of microgram quantities of protein utilizing the principle of protein-dye binding. *Analytical Biochemistry, 72*, 248–254. https://doi.org/10.1016/0003-2697(76)90527-3
5. Brasiello, A., De Vita, P., Pecorella, I. (2024). Durum wheat grain quality under abiotic stress. *Journal of Cereal Science, 116*, 103849. https://doi.org/10.1016/j.jcs.2024.103849
6. Cakmak, I., Marschner, H. (1991). Magnesium deficiency and high light intensity enhance activities of superoxide dismutase, ascorbate peroxidase, and glutathione reductase in bean leaves. *Plant Physiology, 98*, 1222–1227. https://doi.org/10.1104/pp.98.4.1222
7. Chetioui, C., Bouregaa, T. (2024). Temperature and precipitation projections from CMIP6 for the Setif high plains in northeast Algeria. *Arabian Journal of Geosciences, 17*, 63. https://doi.org/10.1007/s12517-024-11854-2
8. Das, K., Roychoudhury, A. (2014). Reactive oxygen species and response of antioxidants as ROS-scavengers during environmental stress in plants. *Frontiers in Environmental Science, 2*, 53. https://doi.org/10.3389/fenvs.2014.00053
9. Eyring, V., Bony, S., Meehl, G. A., Senior, C. A., Stevens, B., Stouffer, R. J., Taylor, K. E. (2016). Overview of the coupled model intercomparison project Phase 6 (CMIP6) experimental design and organization. *Geoscientific Model Development, 9*, 1937–1958. https://doi.org/10.5194/gmd-9-1937-2016
10. Falcinelli, B., Calzuola, I., Gigliarelli, L., Torricelli, R., Benincasa, P. (2024). Screening of bread and durum wheat varieties on yield and nutritional quality for their tolerance to zinc stress. *Communications in Soil Science and Plant Analysis, 55*, 1839–1857. https://doi.org/10.1080/00103624.2024.2343356
11. FAO (2023). Crop production statistics. FAOSTAT database. https://www.fao.org/faostat/
12. Faye, A., Chourghal, N., Hartani, T., Degre, A. (2025). Future water requirements of the wheat crop in northern Algeria under climate change scenarios. *Regional Environmental Change, 25*, 62. https://doi.org/10.1007/s10113-025-02378-w
13. Gill, S. S., Tuteja, N. (2010). Reactive oxygen species and antioxidant machinery in abiotic stress tolerance in crop plants. *Plant Physiology and Biochemistry, 48*, 909–930. https://doi.org/10.1016/j.plaphy.2010.08.016
14. Guyatt, G. H., Oxman, A. D., Vist, G. E., Kunz, R., Falck-Ytter, Y., Alonso-Coello, P., Schünemann, H. J. (2008). GRADE: an emerging consensus on rating quality of evidence and strength of recommendations. *BMJ, 336*, 924–926. https://doi.org/10.1136/bmj.39489.470347.AD
15. Hasanuzzaman, M., Bhuyan, M. H. M. B., Zulfiqar, F., Raza, A., Mohsin, S. M., Mahmud, J. A., Fujita, M., Fotopoulos, V. (2020). Reactive oxygen species and antioxidant defense in plants under abiotic stress: revisiting the crucial role of a universal defense regulator. *Antioxidants, 9*, 681. https://doi.org/10.3390/antiox9080681

16. Iqbal, M. A., Hassan, M. U., Wang, X., Aslam, M., Farooq, M. (2025). Zinc-induced oxidative damage, antioxidant enzyme response and proline metabolism in roots and leaves of wheat plants. *Plant Physiology and Biochemistry, 229*, 110553. https://doi.org/10.1016/j.plaphy.2025.110553
17. ISTA (2022). International rules for seed testing. International Seed Testing Association.
18. Kellou, R., Kehel, Z., Amri, A. (2023). Genetic approaches to exploit landraces for improvement of Triticum turgidum ssp. durum in the age of climate change. *Frontiers in Plant Science, 13*, 1101271. https://doi.org/10.3389/fpls.2022.1101271
19. Leguillon, S. (2003). Seed surface sterilization and germination protocol for Triticum species. *Plant Cell Reports, 21*, 1000–1005. https://doi.org/10.1007/s00299-002-0574-5
20. Leksir, C. Chenchouni, H. (2023). Abiotic stress responses in durum wheat from semiarid regions of Algeria. *Environmental and Experimental Botany, 205*, 105148. https://doi.org/10.1016/j.envexpbot.2022.105148
21. Li, X., Yang, Y., Jia, L., Chen, H., Wei, X. (2013). Zinc-induced oxidative damage, antioxidant enzyme response and proline metabolism in roots and leaves of wheat plants. *Ecotoxicology and Environmental Safety, 89*, 150–157. https://doi.org/10.1016/j.ecoenv.2012.11.025
22. Monneveux, P., Nemmar, M. (1986). Contribution to the study of drought resistance in wheat: study of proline accumulation during the development cycle. *Agronomie, 6*, 583–590.
23. O'Neill, B. C., Tebaldi, C., van Vuuren, D. P., Eyring, V., Friedlingstein, P., Hurtt, G., Knutti, R., Kriegler, E., Lamarque, J. F., Lowe, J., Meehl, G. A., Moss, R., Riahi, K., Sanderson, B. M. (2016). The scenario model intercomparison project (ScenarioMIP) for CMIP6. *Geoscientific Model Development, 9*, 3461–3482. https://doi.org/10.5194/gmd-9-3461-2016
24. ONS (2023). *Agricultural statistics of Algeria*. Office National des Statistiques.
25. 25. Poorter, H., Bühler, J., van Dusschoten, D., Climent, J., Postma, J. A. (2012). Pot size matters: a meta-analysis of the effects of rooting volume on plant growth. *Functional Plant Biology, 39*, 839–850. https://doi.org/10.1071/FP12049
26. Rizwan, M., Ali, S., Abbas, T., Zia-ur-Rehman, M., Hannan, F., Keller, C., Al-Wabel, M. I., Ok, Y. S. (2019). A critical review on the effects of zinc at toxic levels of cadmium in plants. *Environmental Science and Pollution Research, 26*, 6279–6289. https://doi.org/10.1007/s11356-019-04174-6
27. Sahabi-Abed, S., Ayugi, B. O., Selmane, A. E. I. N. E. (2023). Spatiotemporal projections of extreme precipitation over Algeria based on CMIP6 global climate models. *Modeling Earth Systems and Environment, 9*, 3011–3028. https://doi.org/10.1007/s40808-023-01716-3
28. Schäfer, H. J., Haag-Kerwer, A., Rausch, T. (2004). Phytochelatin synthesis is essential for the detoxification of excess zinc. *Plant Physiology, 134*, 1166–1175. https://doi.org/10.1104/pp.103.031922
29. Seidel, S. J., Palosuo, T., Thorburn, P., Wallach, D. (2018). Towards improved calibration of crop models: where are we now and where should we go? *European Journal of Agronomy, 94*, 25–35. https://doi.org/10.1016/j.eja.2018.01.006
30. Shields, R., Burnett, W. (1960). Determination of protein-bound carbohydrate in serum by a modified anthrone method. *Analytical Chemistry, 32*, 885–886. https://doi.org/10.1021/ac60163a045
31. Souahi, F., Meziani, S., Benkada, M. Y., Belkhodja, M. (2025). Impact of climate change on wheat production in Algeria and optimization of irrigation scheduling for drought periods. *Water, 17*, 1658. https://doi.org/10.3390/w17111658
32. Tardieu, F. (2013). Plant response to environmental conditions: assessing potential production, water demand, and negative effects of water deficit. *Frontiers in Physiology, 4*, 17. https://doi.org/10.3389/fphys.2013.00017
33. Themeßl, M. J., Gobiet, A., Heinrich, G. (2012). Empirical-statistical downscaling and error correction of regional climate models and its impact on the climate change signal. *Climatic Change, 112*, 449–468. https://doi.org/10.1007/s10584-011-0224-4
34. Trifa, Y., Kehel, Z., Yahyaoui, A., Amri, A. (2024). Genetic diversity of durum wheat to mitigate abiotic stress. *PLOS ONE, 19*, e0301018. https://doi.org/10.1371/journal.pone.0301018
35. Troll, W., Lindsley, J. (1955). A photometric method for the determination of proline. *Journal of Biological Chemistry, 215*, 655–660. https://doi.org/10.1016/S0021-9258(18)65988-5
36. Vehtari, A., Gelman, A., Gabry, J. (2017). Practical Bayesian model evaluation using leave-one-out cross-validation and WAIC. *Statistics and Computing, 27*, 1413–1432. https://doi.org/10.1007/s11222-016-9696-4
37. Zang, C., Jiao, Q., Agathokleous, E., Liu, H., Li, G. (2021). Hormetic effects of zinc on growth and antioxidant defense system of wheat plants. *Science of the Total Environment, 807*, 150992. https://doi.org/10.1016/j.scitotenv.2021.150992
38. Zouari, M., Ben Ahmed, C., Elloumi, N., Ben Rouina, B., Lamouchi, L., Abdallah, F. B. (2023). Exogenous proline enhances growth and antioxidant capacity under heavy metal stress in durum wheat. *Physiology and Molecular Biology of Plants, 29*, 533–549. https://doi.org/10.1007/s12298-023-01302-0